JOURNAL OF SOLID STATE CHEMISTRY 106, 55–65 (1993)

Palladium Catalyzed Oxidation of Amorphous Carbon: A Study by *in Situ* Transmission Electron Microscopy

H.-I. SU,* K. HEINEMANN,† H. POPPA,‡ AND M. BOUDART§

Department of Chemical Engineering, Stanford University, Stanford, California 94305

Received December 4, 1992; accepted December 23, 1992

IN HONOR OF SIR JOHN MEURIG THOMAS ON HIS 60TH BIRTHDAY

Palladium clusters, 10–30 nm in size, were grown in UHV on amorphous carbon in a transmission electron microscope (TEM). The Pd catalyzed oxidation of carbon was then followed *in situ* in the TEM between 720 and 800 K at a pressure p of O_2 with $0.25 < p\ (10^{-4}\ \text{mbar}) < 1.0$). The behavior of hundreds of individual clusters was recorded on videotape in real time. Clusters moved as they dug irregular channels throughout the carbon film. They exhibited *liquid-like* behavior and frequent change of contrast (*flashing*). These active clusters started to move after an induction period. Some clusters remained inactive. Active clusters coalesced with inactive clusters to form active clusters. After some time, active clusters became and remained inactive. The site time yield of catalyzed oxidation, defined as the number of C atoms reacting per exposed Pd atom per second was almost independent of temperature and proportional to pressure of O_2. Under the conditions of this work, it appears that the rate determining step of the oxidation of carbons is the dissociative chemisorption of O_2 on Pd, with every O_2 molecule sticking to the Pd surface reacting to C with formation of CO_2.

Introduction

The oxidation of carbon has been studied by many investigators. Optical microscopy has been an incisive tool in such studies as pioneered by Thomas (*1*) and Hennig (*2*). In particular, the first microcinematographic record by Thomas and Walker (*3*) of the catalyzed oxidation of carbon provided the first dynamic record of this fascinating phenomenon with catalyst paraticles moving as they consumed carbon by oxidation.

Later on, transmission electron microscopy (TEM) has furthered our understanding of catalyzed oxidation of carbon. In particular, the oxidation of carbon by O_2, catalyzed by particles of metallic palladium, has been studied by controlled atmosphere TEM *in situ*, during the reaction, first by Baker *et al.* in the case of graphite (*4*), and more recently by Penneman and Anton in the case of amorphous carbon (*5*).

In the latter investigation, a turnover rate was reported for the first time, defined as a site time yield (STY), i.e., the number of C atoms oxidized per exposed Pd atom per second. The present work also deals with the Pd catalyzed oxidation of amorphous carbon by O_2. It was undertaken prior to the publication of the work of Penneman and Anton with two purposes in mind: first to follow the phenomenon in real time by *in situ* TEM with recording on videotape,

* *Present address:* Materials Analysis Group, Philips Semiconductors, Mail Stop 65, 811 East Arques Avenue, Sunnyvale, CA 94088.

† ELORET Institute, 1178 Maraschino Drive, Sunnyvale, CA 94086.

‡ IBM–Almaden Research Center, Mail Stop K32/802, 650 Harry Road, San Jose, CA 95120-6099.

§ To whom correspondence should be addressed.

0022-4596/93 $5.00

and second, to measure the rate of catalyzed oxidation quantitatively, i.e., as a STY. We will discuss the comparison between our own work and the previously published work of Penneman and Anton at the end of our paper.

EXPERIMENTAL

Description of the Equipment

As a thorough description of the equipment is given elsewhere (6), only a brief summary of the most important features will be given. The TEM was a Siemens Elmiskop 101 with its original pumps which can reach the low 10^{-6} mbar range. The original equipment was fitted with a second chamber between condenser and objective lenses. This chamber was evacuated by a cryogenic pump to the low 10^{-8} mbar range. A third chamber called the minichamber was pumped by an 80 liter/sec ion-pump and a titanium sublimation pump down to the mid to high 10^{-10} mbar range. The sample was located in the bottom of the minichamber and could be inserted into and removed from the system through an air-lock. The most important features of the system are those of the minichamber. Palladium or other metals could be evaporated inside the minichamber from three sources of metals consisting of metal wires coiled around tungsten filaments. The sample was heated by a tantalum filament located around the sample holder in the bottom of the minichamber, and exposure to different gases within the minichamber was achieved through stainless steel tubing connected to leak-valves.

The possibility of heating the specimen to different temperatures and controlling the flux of evaporated metal during deposition, allowed one to control both the number density of metal particles and their size. A bimodal distribution of particle size was prepared by two successive depositions of metal at different conditions on the same sample. Since experiments were performed *in situ*, uninterrupted observation of the same area of the sample revealed events as they occurred, rather than just before and after reaction.

Temperature calibration was extremely difficult because of the geometry of the system. Thermocouple wires, even very thin ones, could not be used because they transmitted vibrations from the sample introduction system and the cryogenic pump to the sample. Since the sample was located inside the minichamber without any direct line of sight from any of the view-ports into the main chamber, pyrometry could not be used. We managed to calibrate the temperature of the samples indirectly by heating samples of metals (In, Sn, and Pb) *in situ* and recording the heating currents necessary to cause melting of each of the metals. At the melting point of the metals, their diffraction pattern changed from a ring-pattern to a diffuse halo. The maximum achievable sample temperature was ca. 850 K. Although gas exposure was well controlled, the maximum pressure of gas inside the minichamber was about 10^{-4} mbar, because at higher pressures, the pumping speed decreased substantially and the ion pump heated up quickly. Pressure was measured by three ion gauges located in the minichamber, the main chamber, and between the throttle valve and the ion pump. The minichamber ion gauge was not used during the experiments because it generated heat that changed the temperature calibration and also because of the short life of the gauge at the pressure of interest. The pressure during reaction was estimated by comparing the values of the three ion gauges and calculating the conductance of the various chambers and valves. Finally, the resolution of the microscope after the modifications was worse than before because of the lens aberrations introduced by an increase in the distance between the upper and lower pole-pieces of the objective lens, and an increase in the focal length of the objective lens. This increase was due to insertion of differential pumping chambers between the sample and the lower pole-piece of the objective lens. The image intensifier consisted of a micro-

channel plate inserted at the bottom of the camera chamber of the microscope with a phosphor screen underneath both units being *in vacuo*. A video camera, not *in vacuo*, was located under the phosphor screen.

Preparation of Carbon Film

Amorphous carbon films used as support for the Pd particles were prepared in a vacuum system evacuated to 10^{-5} mbar, by arc-evaporation of carbon onto a cleaved mica sheet from spectroscopically pure graphite rods (Ultra Carbon, AGKSP material, Lot No. 125-8-33, with less than 5 ppm maximum allowable total of spot impurities with less than 1 ppm of the following elements: Al, B, Ca, Cr, Cu, Fe, Pb, Mg, Mn, Mo, Ni, Si, Ag, Sn, Ti, W, V, Zn, and Zr). The central portion of the mica sheet, approximately 20 mm in diameter, was shadowed with a metal plate during evaporation, resulting in the deposition of a thinner film of amorphous carbon in that area. The carbon film was then floated off the mica sheet by immersion of the carbon–mica sample in distilled water, picked up by 400 mesh Ni TEM grids, and dried in air. Before they were used to pick-up the carbon films, the Ni grids were cleaned by heating at 10^{-5} mbar until they became red. Without the latter cleaning procedure, unidentified particles appeared on the carbon films upon heating in the minichamber, even before deposition of Pd.

Evaporation of Pd and Reaction in O_2

In a typical experiment, the support film was introduced into the system and heated *in vacuo* (10^{-9} mbar) overnight at a temperature of 700 K. Deposition of Pd was done in two stages. First, the sample was heated to 800 K and left to equilibrate for about one hour, then Pd was deposited. The temperature of the sample was then lowered to 700 K for ½ hr. Then a second deposition with a higher Pd flux was made. This procedure produced a bimodal distribution of Pd particles. In this way, particles of different sizes could be studied at the same time in the same area of the film. After the second deposition, the temperature of the sample was set to the reaction temperature and the sample was exposed to O_2. The behavior of the sample during reaction was recorded in real time on videotape.

RESULTS

Qualitative Observations of the Catalyzed Oxidation

The Pd catalyzed oxidation of amorphous carbon is illustrated by three micrographs of the same area of a sample (Fig. 1a), taken 15 min apart. The white areas in Fig. 1b and 1c are channels where carbon was oxidized away. A metal particle touching the periphery of a channel is responsible for the local formation of that channel by catalytic oxidation of carbon. The Pd particles are inactive at first. Some become active; i.e., they start moving following an induction period of a few minutes after the pressure of O_2 reaches a steady value. Once a Pd particle becomes active, it behaves like a drop of liquid, as its shape changes constantly, and the movement of the particle is accompanied by a pulsation akin to breathing. Particles that are not active in gasification do not exhibit this behavior, which therefore cannot be attributed to the electron beam. As particles move, they collide and coalesce frequently (see Figs. 1a and 1b). When coalescence occurs between an active particle and an inactive one, the resulting particle is generally active. After being active for 15 to 20 min, an active particle suddenly deactivates; i.e., it stops moving. A deactivated paraticle never became active again during our observations. In addition, we never recorded coalescence between an active particle and a deactivated particle. Only a small fraction of the Pd particles was active at a given interval of time. However, after exposure to O_2 at 1.0×10^{-4} mbar for more than 30 min, the major fraction of the particles became active at some point in time, this fraction increasing with time and tempera-

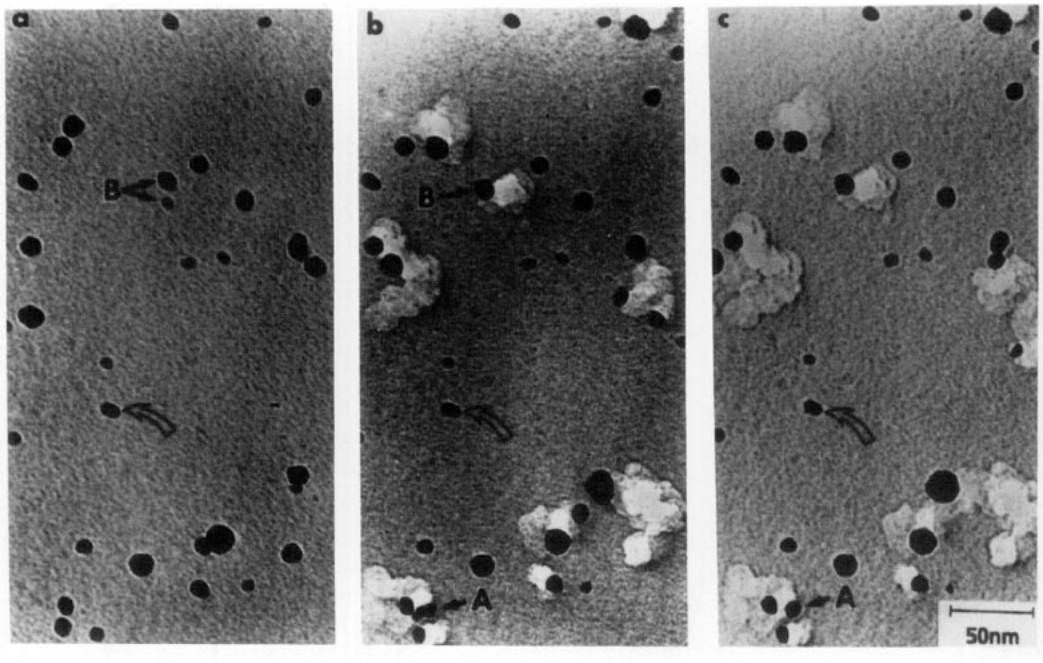

FIG. 1. Channeling Activity: Pd clusters on amorphous carbon. (a) After deposition *in vacuo*. (b) After exposure to O_2 for 15 min at 800 K: the two clusters B in (a) have coalesced. (c) Same after 30 minutes.

ture of reaction. Coalescence of active particles with initially inactive ones was the cause for much of the activity.

After the reaction, different areas of the samples were examined to check for any possible effects of the electron beam. Qualitatively, we could not find any difference between the areas studied continuously under the beam and areas not exposed to the beam during reaction. It is important to point out that the image intensifier present in our *in situ* microscope allowed us to use about $\frac{1}{10}$ of the electron beam intensity normally used for imaging in an electron microscope operating at 100 kV, thus minimizing the effect of electron beam irradiation.

Measurement of the Rate of Catalyzed Oxidation

To measure the rate of carbon oxidation, photographs were taken at regular intervals of time, usually 20 sec, during a playback of the videotape (Fig. 2). Copies of these photographs were made. The areas corresponding to channels formed during a given interval of time were then cut from the copy and weighed. Thus, the change with time of the area of a channel was obtained. To calculate the rate of carbon burnout, the depth of the channels, i.e., the thickness of the films was required.

To estimate the depth of the channels, a sample was submitted after the end of a reaction run to an additional deposition of Pd at room temperature. The smaller clusters so deposited were less than 5 nm in diameter (Fig. 3). The areas in Fig. 3 where no small clusters of Pd can be seen correspond to regions from where carbon was oxidized away completely prior to the additional deposition of Pd. Since the width of a channel corresonds very closely to the diameter of the active Pd cluster that produced the channel, the diameter of the smallest Pd clusters to perforate the carbon

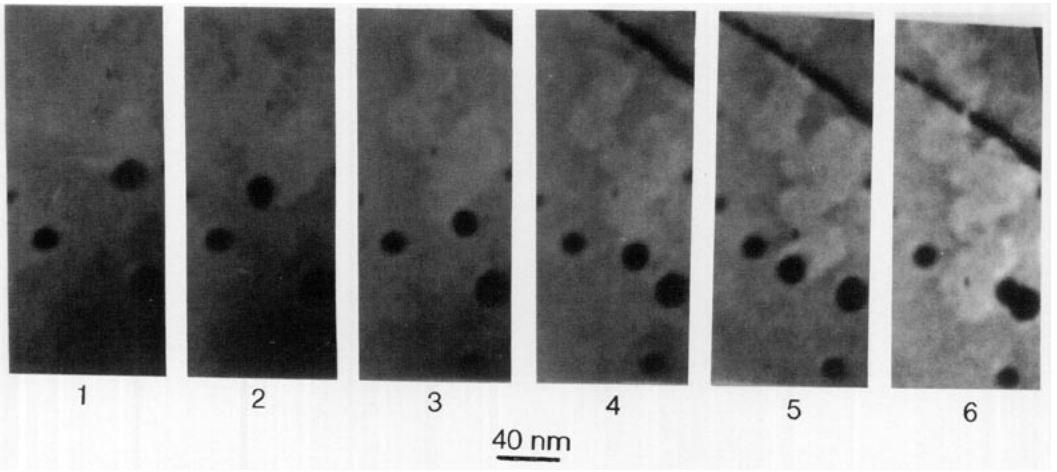

FIG. 2. A typical time sequence used for the quantitative measurement of the rate of C oxidation.

film was assumed to be equal to its thickness. These clusters were roughly 10 ± 3 nm in diameter. Hence the thickness of the film, corresponding to the depth of the channels, was assumed to be 10 nm.

The diameter of an active Pd cluster was measured directly from the photographs. Since the shape of a cluster changed with time in an irregular way, the size of a given cluster was measured whenever possible from four different photographs of a given sequence, as shown in Fig. 2. Furthermore,

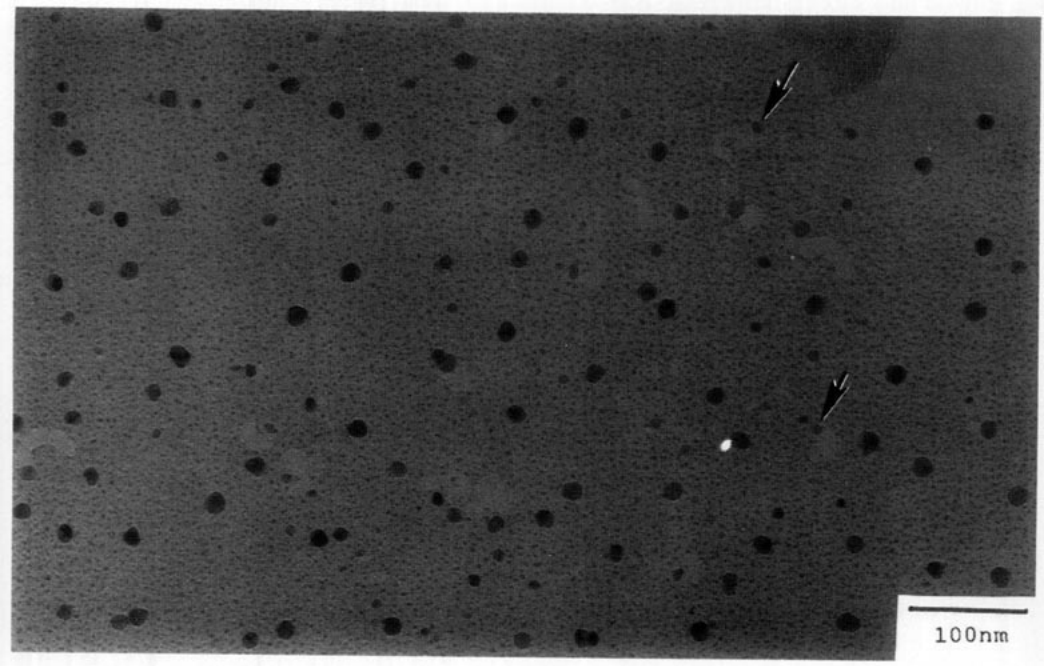

FIG. 3. Pd clusters of amorphous carbon after a second deposition of Pd following an oxidation run. Clusters with arrows are roughly 10 nm in diameter and perforated the carbon film.

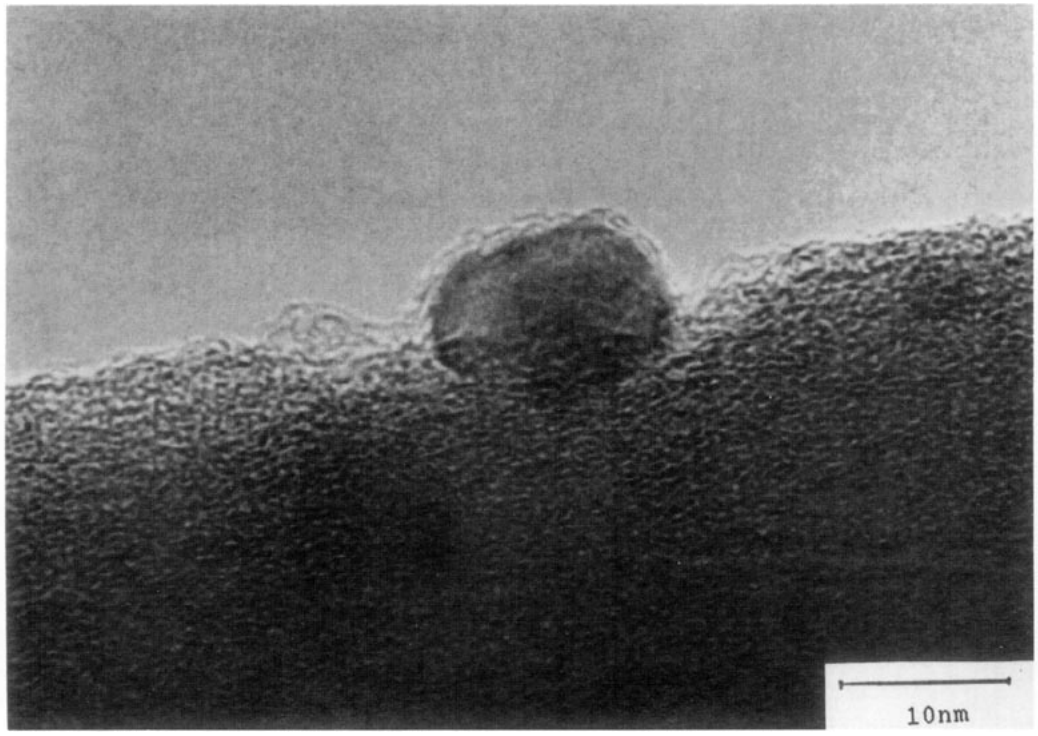

FIG. 4. Pd cluster in profile.

the longest and shortest dimensions of each cluster were averaged. Then, the shape of the particles was assumed to be spherical as revealed by micrographs of particles in profile, taken *ex situ* in a JEOL 2000EX after completion of the gasification experiment (Fig. 4). Two other quantities were used in the calculation of the rates. The number of Pd atoms on the surface of Pd was taken to be 1.5×10^{15} atoms cm^{-2}, the average number density of Pd atoms on low index planes of Pd, and the value 1.8 was used as the specific gravity of amorphous carbon (7). With these values, the rate of reaction, i.e., number of C atoms reacted per second per cluster, could be calculated for each run as a function of the total number of surface Pd atoms per cluster (Figs. 5a–5c).

DISCUSSION

Behavior of Pd Clusters during Gasification of Carbon

After exposure to O_2, reaction starts at the few contact points between Pd clusters and amorphous carbon. In a matter of minutes the cluster digs itself into the film until an extended interface between the oxidized Pd surface is formed and the cluster becomes active. The length of this induction period depends on the original contact between the cluster and the originally rough surface of the carbon film

After formation of the interface, CO and CO_2 are produced and removed by diffusion through the pores of the carbon film. Our observations *in situ* show that, at irregular intervals, the cluster momentarily loses contact with the carbon film. The cluster rotates in a jerky motion to form a new interface between a freshly oxidized area of the metal and the carbon film. This rotation explains the flashing or frequent change in contrast of the Pd cluster as it moved. Flashing was not periodic, although clusters that propagated faster did show more rapid rates of change in contrast. The Pd particles changed contrast more frequently also when their trajectories were deviating from a

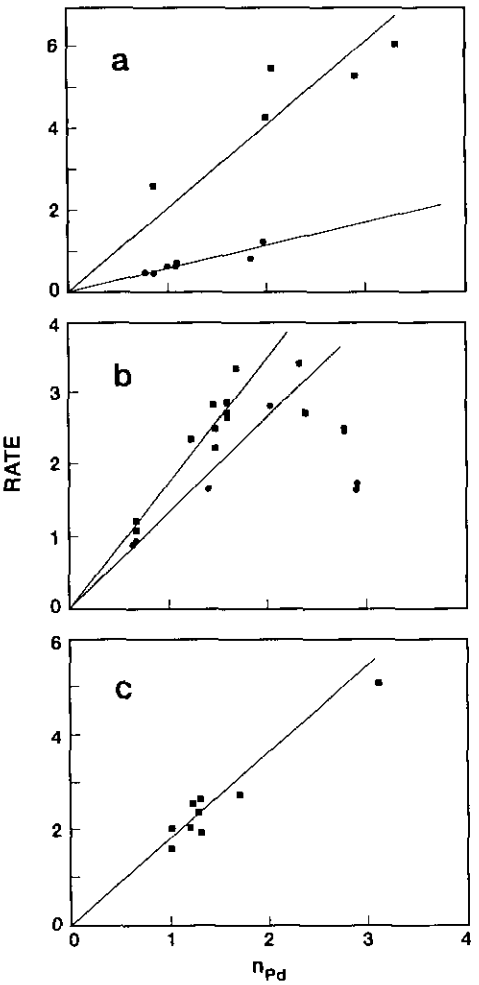

FIG. 5. Rate vs n_{Pd}. Rate (10^4 C atoms oxidized per second per cluster). n_{Pd} (10^4 Pd atoms per cluster). (a) 800 K, ● $P_{O_2} = 2.5 \times 10^{-5}$ mbar; ■ $P_{O_2} = 1.0 \times 10^{-4}$ mbar. (b) 750 K, ● $P_{O_2} = 0.8 \times 10^{-4}$ mbar; ■ $P_{O_2} = 1.0 \times 10^{-4}$ mbar. (c) 720 K, ■ $P_{O_2} = 1.0 \times 10^{-4}$ mbar.

straight line. Since diffraction contrast is the predominant mechanism of contrast under our conditions, the frequent change in contrast of the Pd particles is logically ascribed to changes in particle orientation, resulting in different diffraction conditions. The reorientation of the Pd cluster may perhaps be related to crystalline anisotropy of the metal. Indeed, Moorhead *et al.* (*8*) have observed that the direction of the channels etched by Pd clusters during Pd catalyzed gasification of amorphous carbon was not random. Rather, ca. 75% of the clusters seemed to move in high index directions of Pd.

Three more consequences of the formation of an active interface between surface oxidized clusters and the carbon film should be pointed out.

The first is the liquid-like behavior of the active clusters. It has been suggested that Pd is in the liquid phase during reaction as its exothermicity increases the temperature of the clusters above the melting point (*9*). However, as we have observed Bragg diffraction contrast of active clusters in the TEM, these clusters must be crystalline. The liquid-like behavior is probably due to *wetting* of the support by Pd clusters covered with oxygen, because oxidized metals interact strongly with supports (*10*) as clusters rotate.

Second, the high interfacial energy of the contact between surface oxidized metal and support may explain why the Pd clusters remain on the carbon support in our experiments although they carve channels through the carbon film. If O atoms at the Pd/C interface react with carbon atoms, eventually the Pd particles might lose contact with the carbon film and fall, even if O atoms diffuse back to the Pd/C interface. However, flashing and the liquid-like behavior of the Pd particles indicate that the clusters rotate so as to wet the carbon support as the clusters propagate. Thus when a Pd cluster loses contact with the support due to consumption of carbon and oxygen, another part of the surface oxidized cluster quickly reestablishes contact with the carbon film.

A third manifestation of the active interface is the repeated observation that coalescence between an active cluster and an inactive one yields an active larger cluster: the active interface on the active cluster continues the reaction.

Two questions remain: first, how does the oxygen reach the active interface? This will be considered in the next section pertaining to the quantitative measurement of the rate of oxidation.

TABLE I

NUMBER OF C ATOMS REACTED PER SECOND PER Pd ATOM EXPOSED

Temperature (K)	Pressure of O_2 ($\times 10^{-4}$ mbar)	v_1 (sec^{-1})
800	0.25	0.6
800	1.0	2.0
750	1.0	1.7
750	0.8	1.3
720	1.0	1.7

The second question is: why does an active cluster cease to be active after a while and remain inactive afterward? The first thought is that a cluster collects impurities in the carbon film as it channels through it until the Pd surface becomes poisoned. But this explanation can be ruled out. Indeed, a typical 20-nm cluster exposes $\sim 2 \times 10^4$ Pd atoms. If it dies after, say, 2×10^3 sec, each surface Pd atom will have oxidized $\sim 4 \times 10^3$ C atoms (see Table I). Thus the whole cluster surface will have oxidized $4 \times 10^3 \times 2 \times 10^4 \sim 10^8$ C atoms. With impurities in the film totaling 5 ppm, the cluster would have collected ~500 impurity atoms covering less than 3% of its surface. Another possibility is that the Pd surface becomes progressively covered with graphitic or amorphous carbon until it ceases to be active. There is ample evidence to support such a possibility, albeit under conditions different from those used in this work. Thus diffusion of carbon through the bulk of metals has been studied extensively. The growth of filamentous carbon on catalyst particles, especially Fe, Ni, and Co, during exposure to carbon containing gases, such as CH_4 and acetylene at temperatures ranging from 575 to 975 K is well documented (*11–13*) and demonstrates that carbon can diffuse at appreciable rates through metal particles.

Moreover, the possibility of carbon–carbon bonds dissociating as a result of catalysis by Pd has been demonstrated before, but not in the same temperature range as the one employed in these experiments. Holstein *et al.* (*14*) observed by *in situ* TEM that Pd catalyzes the graphitization of amorphous carbon at 1150 K *in vacuo* by a solution-precipitation mechanism consisting of dissolution of carbon into the bulk of a catalyst and subsequent precipitation of graphitic carbon. Catalyzed graphitization by the solution-precipitation mechanism requires that carbon–carbon bonds are dissociated.

A recent study of the interaction of Pd clusters with amorphous carbon (*15*) suggests that Pd catalyzed dissociation of carbon–carbon bonds can occur at temperatures as low as 870 K, with formation of amorphous layers of material around the Pd particles. Yet these layers may have formed on Pd clusters as a result of contamination in air, followed by irradiation by high energy electron beams in a non-UHV electron microscope.

This led us to examine our samples after the gasification reaction by high resolution TEM. High resolution electron microscopy of a sample treated in 1×10^{-4} mbar of O_2 at approximately 900 K (*16*) shows the presence of a layer of material at the back of the active Pd particle, i.e., at the side opposite that of carbon consumption (Fig. 6). The ratio between the lattice spacing of this material and that of Pd(111) in the same micrograph is 1.5, which is very close to the ratio of d-spacings of graphite (002) (d = 335 pm) to Pd(111) (d = 224 pm). The smaller particles in this micrograph are Pd clusters that were deposited at room temperature after the *in situ* experiment was completed. In other experiments, many of the active clusters had layers of material behind them, but there were fewer layers and these layers did not seem to be ordered, since high resolution TEM was done with a JEOL 2000EX microscope operating at 200 kV. As mentioned above, it is possible that the appearance of amorphous carbon was due to contamination in air prior to insertion into the TEM, followed by interaction with residual gases under the high energy electron beam. Thus, at the moment, the carbon contamination of Pd clusters remains a likely but not a conclu-

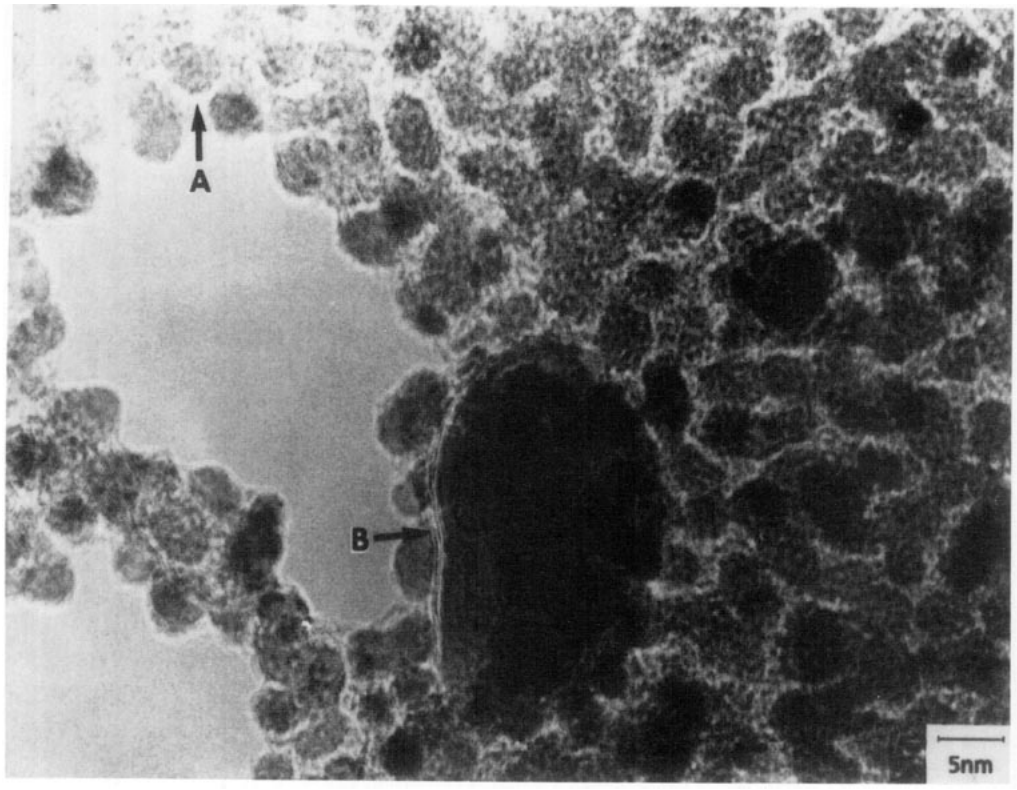

FIG. 6. Sample of Pd clusters on amorphous carbon after an oxidation run. (a) A small cluster deposited in vacuo after the reaction. (b) A large cluster exhibiting layers of graphitic carbon.

sive explanation for the cessation of their activity.

Rate of Palladium Catalyzed Oxidation of Carbon: Site Time Yield

In Figs. 5a–5c, the plots are linear. The slope of each plot is a site time yield (STY), i.e., the number of carbon atoms oxidized per Pd atom per second. The value of the STY does not depend on the nature of the product of carbon oxidation, CO or CO_2. The values of STY collected in Table 1 are 1.7, 1.7, and 2.0 at 720, 750 and 800 K, respectively, and at constant pressure of O_2, 1.0 mbar. Thus values of STY are essentially temperature independent between 720 and 800 K. At 800 K, an increase in pressure by a factor of 4 increases STY values by a factor of 3.3. At 750 K, an increase in pressure by a factor of 1.25 increases the STY by a factor of 1.33. Thus it appears that STY is proportional to O_2 pressure. The latter conclusion was also reached in a much more convincing manner by Penneman and Anton at 795 K with pressures of O_2 between 5×10^{-7} and 1×10^{-5} mbar (*5*). These authors studied the Pd catalyzed oxidation of amorphous carbon films, 10–20 nm in thickness produced *ex situ* in a manner similar to ours. Palladium clusters, 15–20 nm, were grown *in situ* in a Philips EM 400 TEM equipped with a bakeable UHV chamber with a base pressure of 8×10^{-9} mbar pumped by a turbomolecular pump. Two Knudsen-type cells were used with a substrate temperature of 680 K.

In their calculation of STY, Penneman and Anton used the projected area of Pd clusters. By extrapolation of their linear plot

of STY vs O_2 pressure to 1.0×10^{-4} mbar at 795 K, we find a STY value of 4 sec^{-1}, to be compared to our value of 2 sec^{-1} at the same pressure and 800 K (Table I). The agreement is striking. A detailed comparison cannot be made, as the authors did not describe the method by which the STY was obtained. But it must be noted that the authors report an activation energy of 65 kJ $mole^{-1}$ from an Arrhenius plot *below* 700 K, while *above* 700 K the Arrhenius line bends over and the activation energy becomes very small, down to 5 kJ $mole^{-1}$, in agreement with our finding that STY values are essentially independent of temperature between 720 and 800 K (Table I).

Mechanism of the Pd Catalyzed Oxidation of Amorphous Carbon

The results of Penneman and Anton (*5*) and our own suggest a mechanism on the basis of both qualitative and quantitative observations *in situ* in the TEM. As usual, it is not *the* mechanism but *a* mechanism for temperatures above 700 K and pressures of O_2 between 5×10^{-7} and 1.0×10^{-4} mbar, with Pd clusters between 10 and 30 nm in size supported on C films ca. 10 nm thick.

The most incisive quantitative result is that, for the conditions just listed, the Pd site time yield is proportional to pressure of O_2.

The simplest mechanism involves three one-way (i.e., irreversible) elementary steps in the catalytic cycle:

$$O_2 + 2^* \rightarrow 2O^* \quad (1)$$

$$O^* \rightsquigarrow (O^*)_i \quad (2)$$

$$(2O^*)_i + C \rightarrow CO_2 + 2^*. \quad (3)$$

The first step is the dissociative chemisorption of O_2 on two Pd sites denoted by *; this step may be taking place through a surface precursor state. The second step represents surface diffusion of O atoms chemisorbed on Pd to the interface (denoted by subscript i) between surface oxidized Pd and the amorphous carbon film as discussed in the qualitative section of the discussion. The third step is the reaction between O* with C to form CO_2; this step may also proceed in two substeps.

Since the STY is first order in pressure of O_2, the rate determining step in the sense discussed elsewhere (*17*) must be the first step. Moreover, the first step must take place on a Pd surface sparsely covered with O* to obtain first order behavior. Thus the mechanism is very simple, provided that oxygen atoms can diffuse on Pd clusters over a distance less than 15 nm during one turnover time of the order of 1 sec. This is feasible if the diffusion coefficient D is of the order of 10^{12} cm^2 sec^{-1} as estimated from Einstein's equation. This is close to the value of D for atomic O on W(110) at 800 K as obtained from the data of Tringides and Gomer (*18*) as reported by Baetzold (*19*). Since the binding energy of O on W is much higher than on Pd, the value of D should be much larger on Pd than on W at the same temperature. Hence it is reasonable to expect that O atoms chemisorbed on the clusters of the size used in this work can diffuse rapidly to the Pd/C interface where they react with carbon. Thus, the steady-state surface concentration of O atoms on the free surface of the clusters remains small as indicated by the kinetics.

Another check of the mechanism is based on the fact that the rate of chemisorption of O_2 on Pd must be equal at the steady state to the measured rate of oxidation of carbon. In turn, the rate of chemisorption of O_2 on C must be equal to the areal rate of collision r_c of O_2 molecules on the free Pd surface times the sticking probability σ of O_2 on Pd at low surface coverage.

From the data of Table I, since the STY value at 800 K and 1.0×10^{-4} mbar is 2 sec^{-1} the areal rate r_o of carbon oxidation is $2 \times 1.5 \times 10^{15} = 3 \times 10^{15}$ cm^{-2} s^{-1}. Now the Pd catalyzed oxidation of C probably leads to CO_2 (*20*) since Pd is an excellent catalyst for CO oxidation (*21*). Then $r_c = r_o$ at the same pressure and temperature. From gas kinetic theory, $r_c \sim 10^{19}$ cm^{-2} sec^{-1}.

Hence σ is of the order of 10^{-4} to 10^{-3}. As it is well known that the chemisorption of O_2 is not activated, this value of σ for the dissociative chemisorption of O_2 through a localized transition state is reasonable (*22*), although it is in strong disagreement with the value of 0.2 reported for σ on Pd(111) at 800 K (*23*). The reason for this discrepancy is not clear.

CONCLUSION

The work of Penneman and Anton and our work provide qualitative and quantitative evidence for the mechanism of Pd catalyzed oxidation of amorphous carbon at low pressures of O_2 ($\sim 10^{-4}$ mbar) and high temperatures ($700 < T(K) < 800$). The proposed mechanism is that O_2 dissociates on the free surface of the Pd clusters to yield atomic O that diffuses rapidly on the Pd surface to an active interface between the surface oxidized metal and the carbon film of a thickness comparable to the size of the clusters.

This mechanism is similar to one proposed for the Pt catalyzed oxidation of high surface area carbon by nitric oxide (*24*). It was proposed that NO dissociates on the Pt clusters to yield O atoms that diffuse to the Pt/C interface where CO and CO_2 are formed. At the same time, N atoms recombine on Pt at a rate equal to that measured separately by others (*25*). It would be interesting to observe such a system by *in situ* TEM.

Acknowledgments

The authors acknowledge the support of NASA Grant NCC 2-394 and DOE Grant DE-FG03-87ER13762 and thank Miguel Avalos-Borja for taking the micrographs shown in Figs. 4 and 6, and Dr. Fernando Ponce for our use of TEM at the Palo Alto Research Center of Xerox.

References

1. J. M. THOMAS, *Chem. Phys. Carbon* **1,** 121 (1965).
2. G. R. HENNIG, *Chem. Phys. Carbon* **2,** 1 (1966).
3. J. M. THOMAS AND P. L. WALKER, JR., "First Symposium on Carbon," Tokyo (1964).
4. R. T. K. BAKER, J. A. FRANCE, L. ROUSE, AND R. J. WAITE, *J. Catal.* **41,** 22 (1976).
5. B. PENNEMAN AND R. ANTON, *J. Catal.* **118,** 417 (1989).
6. K. HEINEMANN AND H. POPPA, *J. Vac. Sci. Technol. A* **4,** 127 (1985).
7. Handbook of Physics and Chemistry, CRC Press, 1990.
8. R. D. MOORHEAD, K. H. HEINEMANN, AND H. POPPA, *J. Vac. Sci. Technol.* **17,** 248 (1980).
9. J. R. FRYER, *Nature* **220,** 1121 (1968).
10. E. RUCKENSTEIN AND Y. F. CHU, *J. Catal.* **59,** 109 (1979).
11. R. T. K. BAKER, M. A. BARBER, F. S. FEATES, P. S. HARRIS, AND R. J. WHITE, *J. Catal.* **26,** 51 (1972).
12. J. L. FIGUEREDO, C. A. BERNARDO, J. J. CHLUDZINSKI, AND R. T. K. BAKER, *J. Catal.* **110,** 127 (1988).
13. R. T. YANG AND J. P. CHEN, *J. Catal.* **115,** 52 (1989).
14. W. L. HOLSTEIN, R. D. MOORHEAD, H. POPPA, AND M. BOUDART, *Chem. Phys. Carbon* **18,** 139 (1982).
15. R. LAMBER, N. JAEGER, AND G. SCHULZ-EKLOFF, *Surf. Sci.* **227,** 15 (1990).
16. H.-I. SU, Ph.D. dissertation, Chapter IV, Stanford University.
17. M. BOUDART AND K. TAMARU, *Catal. Lett.* **9,** 15 (1991).
18. M. TRINGIDES, AND R. GOMER, *Surf. Sci.* **145,** 121 (1984).
19. R. C. BAETZOLD, *in* "Metal–Surface Reaction Energetics" (E. Shustorovich, Ed.), p. 114, VCH, New York (1992).
20. C. HEUCHAMPS AND X. DUVAL, *Carbon* **4,** 243 (1966).
21. T. ENGEL AND G. ERTL, *Adv. Catal.* **28,** 1 (1979).
22. M. BOUDART AND G. DJÉGA-MARIADASSOU, "Kinetics of Heterogeneous Catalytic Reactions," *Princeton Univ. Press, Princeton, NJ (1984).*
23. T. ENGEL, *J. Chem. Phys.* **69,** 373 (1978).
24. K. J. LIM, D. G. LÖFFLER, AND M. BOUDART, *J. Catal.* **100,** 158 (1986).
25. K. J. LIM AND M. BOUDART, *J. Catal.* **105,** 263 (1987).